

Copyright 2004 Society of Photo Instrumentation Engineers.

This paper was published in SPIE Proceedings, Volume 5553 and is made available as an electronic reprint with permission of SPIE. One print or electronic copy may be made for personal use only. Systemic or multiple reproduction, distribution to multiple locations via electronic or other means, duplication of any material in this paper for a fee or for commercial purposes, or modification of the content of the paper are prohibited.

Improving spatial light modulator performance through phase compensation

Jamie Harriman, Anna Linnenberger, and Steve Serati
Boulder Nonlinear Systems, Inc.
450 Courtney Way, #107
Lafayette, Colorado 80026

ABSTRACT

High-resolution, liquid-crystal spatial light modulators (SLMs) are being used as dynamic phase screens^{1,2} for testing optical systems and as optical wavefront compensators^{3,4} to dynamically correct distortions. An SLM provides hundreds of waves of adjustable phase modulation across the aperture of the device. Some of this phase adjustment can be used to compensate for distortions internal to the SLM such as backplane curvature. Because of modulo- 2π operation, the dynamic range of the device is not significantly decreased by adding phase compensation, as long as the phase shift over the aperture is only a few waves. In this paper, we will discuss the techniques being used to determine the correct phase compensation for SLMs and how the compensation is being applied through the SLM control software.

Keywords: phase compensation, spatial light modulator, phase screens, wavefront compensation

1. INTRODUCTION

High-resolution phase-only SLMs generate phase profiles with hundreds of waves of stroke using modulo- 2π modulation. However, there are several implementation issues that prevent this capability from being easily realized when SLMs are integrated into systems as wavefront controllers. One problem is that display-type metrics have been traditionally used to characterize and calibrate phase SLMs, instead of metrics based on wavefront quality and accuracy of the phase profiles that are generated. The use of display metrics for evaluating phase SLM performance has resulted in incomplete calibration for phase screen generators and wavefront compensators, forcing additional characterization by the end user.^{5,6} To help solve this problem, Boulder Nonlinear Systems (BNS) is taking a leadership role in defining new metrics to evaluate Liquid Crystal on Silicon (LCoS) Spatial Light Modulators (SLMs) used as wavefront controllers. In this effort to more accurately characterize and calibrate phase-only SLMs, new testing and calibration methods are being developed as well as new control software that will allow users to correct static aberrations within the system while dynamically varying the phase profile using Zernike Polynomial Coefficients to control the phase front.

LCoS SLMs have an inherent curvature to them causing reflective wavefront distortion in an optical system. The silicon backplanes used in LCoS SLMs are one of the largest contributors to the curvature of an SLM due to limitations in the polishing process at silicon foundries. The liquid crystal layer also contributes to the reflected wavefront distortion. The total wavefront distortion in an optical system that uses an LCoS SLM, is the sum of the reflected wavefront distortion due to the SLM and the wavefront distortion cause by all of the other components in the system. In a phase only optical system this wavefront distortion causes phase error. Since phase SLMs can be used to compensate for unwanted phase error, the devices can be self correcting. The phase error due to the distortion of a device can be greatly reduced through a wavefront distortion analysis and calibration procedure. Fortunately, the phase error compensation does not significantly reduce the dynamic range of the SLM as long as there are less than a few waves of distortion across a device.

The wavefront distortion analysis and compensation procedure includes a fringe analysis of the SLM using an interferometer (refer to Figure 4). This fringe analysis produces Zernike Polynomial Coefficients which describe the

wavefront distortion across the active area of the device. Zernike polynomials are only orthogonal functions when representing circular apertures that have no discontinuity within the aperture. Because of the circular nature of the Zernike polynomials, the compensation of the corners of the square SLM aperture is limited.

The wavefront compensation application requires that the devices have a linear phase response. Because the LCoS SLM devices do not have a linear phase response using gray values that linearly increase from 0 to 255 (for an 8 bit system), the device must be calibrated. This calibration is the second step in the wavefront distortion calibration and compensation and results in a look up table (LUT) for a device. The LUT calibration defines a mapping of 0 to 255 grayscale values to a new set of grayscale values that result in a linear phase response of the device over a full wave, 0 to 2π , of stroke. The LUT calibration is critical because the wavefront distortion compensation is applied to the SLM modulo- 2π . Therefore, the optimum gray levels for 0 and 2π must be determined so that the transitions between them are smooth. If the optimum values for 0 and 2π phase are not used, there can be unwanted phase modulation in the 0 to 2π transitions.

The third step is the application of the wavefront distortion compensation to the SLM. After the wavefront distortion calibration is complete, the SLM control software application can be used to write phase patterns to the SLM while applying the compensation to the SLM. Since the compensation is added to the desired phase pattern using modulo- 2π addition, it does not significantly reduce the dynamic range of the SLM, which has effectively hundreds of waves of stroke.

The interferograms shown in Figure 1 and Figure 2 illustrate an example of a 512 x 512 phase SLM before and after wavefront distortion compensation. The wavefront distortion before compensation was approximately 1.2λ at 690nm (refer to Figure 1). The wavefront distortion after compensation is approximately $\lambda/4$ at 690nm and is shown in Figure 2.

Device 1 before wavefront distortion compensation ~ 1.2λ (1.2 waves) analyzed over a square aperture

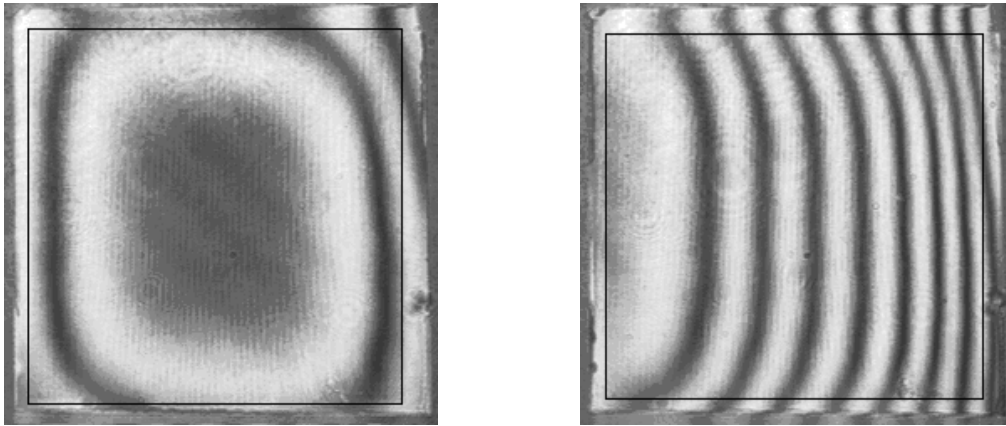


Figure 1. 512 x 512 SLM, Device 1 before wavefront distortion compensation with no tilt (left) and x-tilt (right). The wavefront distortion of this device is approximately 1.2λ (1.2 waves) at 690nm.

Device 1 after wavefront distortion compensation ~ 1/4 (.25 waves) analyzed over a circular aperture

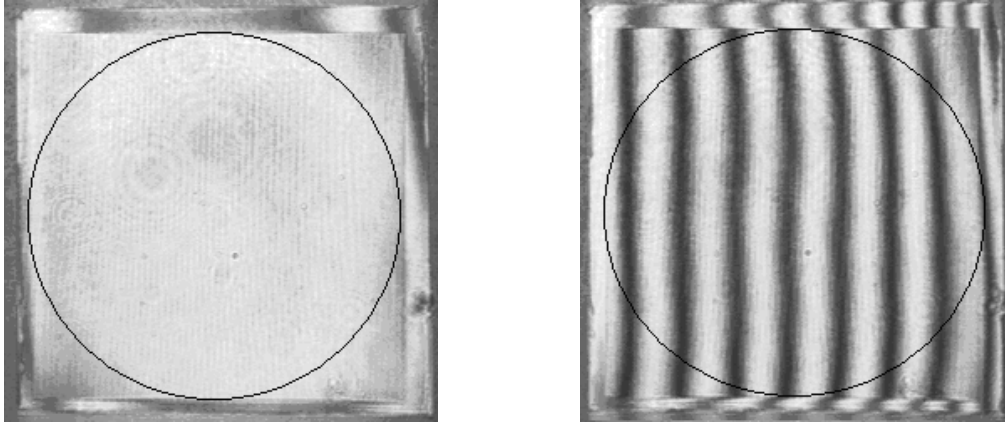


Figure 2. 512 x 512 SLM, Device 1, after wavefront distortion compensation with no tilt (left) and x-tilt (right). The wavefront distortion of this device is approximately 1/4 (1/4 wave) analyzed over a circular aperture at 690nm.

The phase SLM calibration software shown in Figure 3 below can be used to automatically generate the look up table (LUT) for a device. The calibration software also reads in the 20 Zernike Polynomials generated by the fringe analysis software. Using the Zernike Polynomials and the LUT, a compensation image is created and can then be applied to the SLM. The compensation image and LUT can then be saved for use with the SLM control software.

Phase SLM Characterization and LUT Generation - Fringe Center

Test Wavelength: 690 Design Wavelength: 690

Fringe Analysis File (.qtd)

File Name: slm5899n_atRed Pre Corr P-V Error: 1.16128

Post Correction File Name: slm5899n_atRed Post Corr P-V Error: 0.233009

Saving

Corr Image File Name: slm5899n.bmp SLM Serial Number: slm5899n

LUT File Name: slm5899n.LUT

Min Valley Value: 130 Generate LUT Align

Bitmap: no file Superimpose

Zernike Polynomials - Correction Image			
Piston	Coma X	Second Astig Y	Tert. Spherical
0 0	6 -0.0272822	12 0.00181688	24 0.00293942
X Tilt	Coma Y	Second Coma X	Quat. Spherical
1 -6.02724	7 0.0339512	13 0.0158729	35 0
Y Tilt	Spherical	Second Coma Y	
2 0.210124	8 -0.309868	14 -0.0354975	
Power	Trefoil X	Second Spherical	
3 -1.21297	9 0.0852891	15 0.0213875	
Astig X	Trefoil Y	Tetrafoil X	
4 -1.05513	10 0.0583897	16 -0.715677	
Astig Y	Second Astig X	Tetrafoil Y	
5 0.236726	11 -0.392365	17 -0.0142471	

Figure 3. Calibration software application reads in Zernike Polynomials, calibrates a LUT, creates a compensation image for an SLM

2. FRINGE ANALYSIS

The first step in analyzing wavefront distortion on an LCoS SLM is fringe analysis. Using a Michelson interferometer as shown in Figure 4, the reflected wavefront distortion of the SLM & optical system is measured by analyzing the interference fringes. As the X, Y, or XY tilt is added multiple fringes across the aperture can be seen. The degree of curvature of these interference fringes describes the severity of the wavefront distortion. The less the wavefront distortion, the straighter the fringes will be. An image of the fringe pattern created by the SLM is captured using a frame grabber. This image is then analyzed using a software program that calculates the Zernike coefficients based on the fringe pattern. The consistency and accuracy of the interferometer setup is critical for repeatable and consistent fringe analysis.

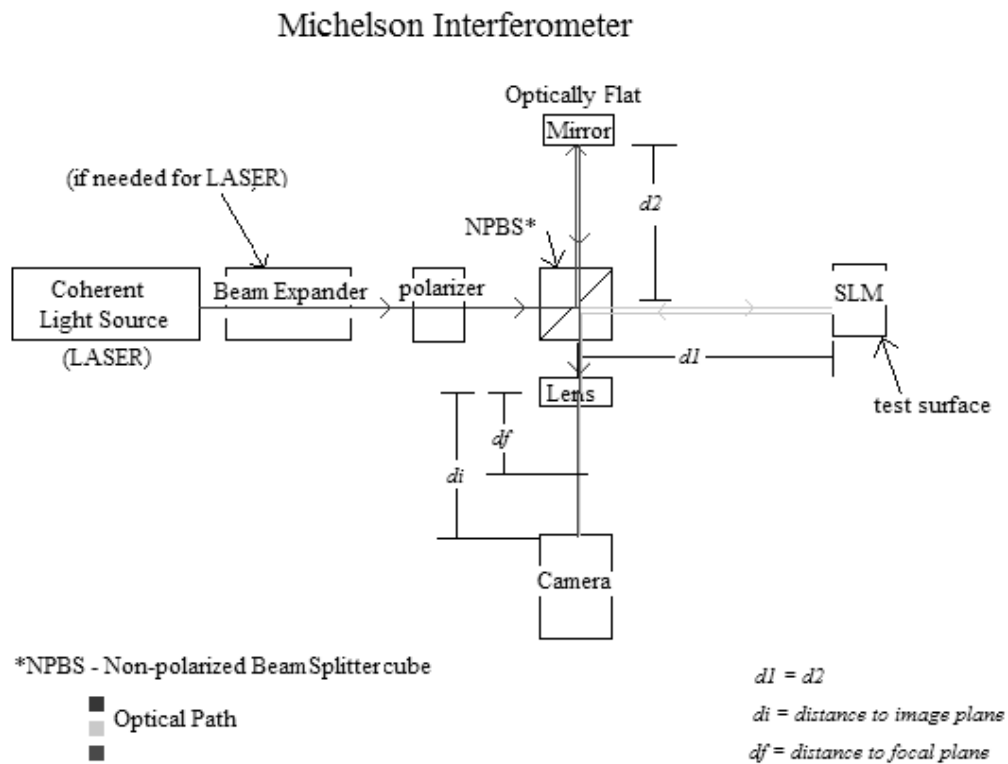


Figure 4. Michelson Interferometer – optical setup for measuring wavefront distortion of the SLM and optical system

3. WAVEFRONT DISTORTION AND ZERNIKE POLYNOMIALS

In the calibration, Zernike Polynomials 0 through 17, 24 and 35 are used to define the wavefront distortion through fringe analysis. However, through testing, it was found that the most significant Zernike polynomials were Power, Astigmatism X, and Astigmatism Y which are illustrated in Figure 5. These three Zernike Polynomials alone achieve approximately 65% of the total compensation. Each higher order Zernike polynomial following these three helps to slightly improve the overall compensation.

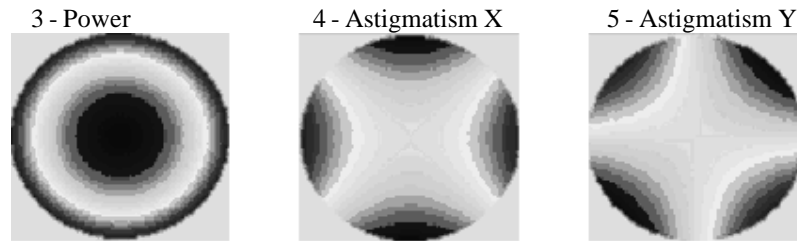


Figure 5 The third, fourth, and fifth Zernike Polynomials, Power, Astigmatism X and Astigmatism Y contribute approximately 65% of the total compensation of a device (illustrations courtesy of Scott Harris of Mission Research Corporation).

4. LOOK UP TABLES (LUTs)

Another important part of the wavefront distortion calibration is the LUT calibration. In a phase-only SLM application a LUT is used to map grayscale values 0 to 255 to a new set of grayscale values that result in a linear 0 to 2π phase shift. If the mapping is correct, then gray value 0 should be mapped to a grayscale value that will result in a 0 phase shift, gray value 64 should be mapped to a grayscale value that will result in a $\pi/2$ phase shift, gray value 128 should be mapped to a grayscale value that will result in a π phase shift and so on up to gray value 255 mapping to a grayscale value that will result in a 2π phase shift.

One technique of translating grayscale values to phase shifts uses a series of 128 images. Each of these 128 images is applied to the SLM and then the resulting image is frame grabbed and analyzed. The series of 128 images that are applied to the SLM all have a grayscale value of 0 on the top half of the image, which acts as the reference, and have an incrementing grayscale value on the bottom half of the image. The first image has a grayscale value of 0 on the top, and a grayscale value of 0 on the bottom. The next image has a grayscale value of 0 on the top, and a grayscale value of 1 on the bottom. The images continue to increment in the grayscale value along the bottom of the image until the last image, which has a grayscale value of 0 on the top and a grayscale value of 127 on the bottom. The left side of Figure 7 shows an example image, which has a grayscale value of 0 on the top and a grayscale value of 55 on the bottom. The right side of Figure 7 shows the frame grabbed data that was stored when the image on the left was applied to the SLM. This figure illustrates that a grayscale value of 55 results in approximately a π phase shift, because the fringes along the bottom half of the SLM are approximately shifted by 50 percent of the distance between the fringes along the top half of the SLM.

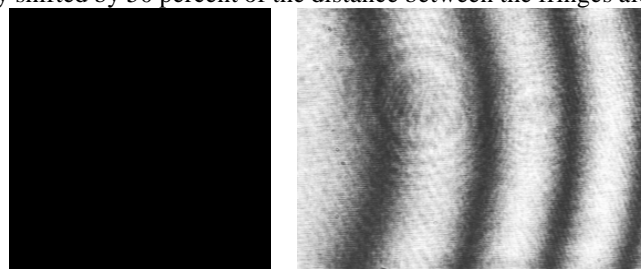


Figure 6 Grayscale 0 (left), result (right) 0 phase shift

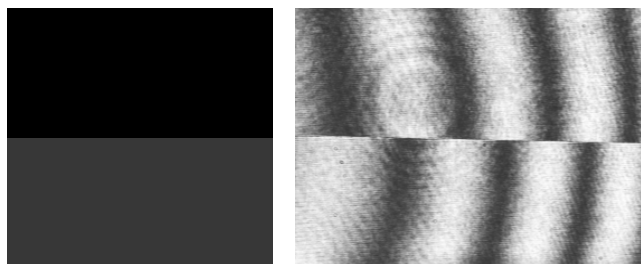


Figure 7 Grayscale 55 (left), result (right) π phase shift

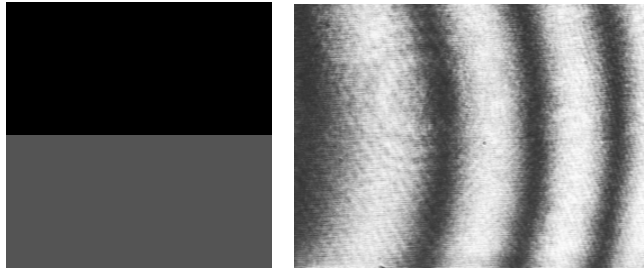


Figure 8 Grayscale 77 (left), result (right) 2π phase shift

This process of generating a LUT can be quiet tedious, time consuming, and potentially less accurate if implemented manually. As a more efficient and consistent alternative, a program has been written that automatically computes the phase shift that is produced by each gray value. The images describe above are loaded onto the SLM, and the resulting phase patterns are captured and analyzed. The analysis program automatically calculates the phase shift that results from each gray value with respect to a 0 phase shift. The output of this analysis is a LUT that maps gray values 0 to 255 to the gray values that give a linear phase shift over a full wave (0 to 2π) of phase stroke. This program is included in the calibration software application (refer to Figure 3).

In the SLM system discussed in this section, the electrical addressing scheme uses 8 bits or 256 gray levels. However, as mentioned earlier in this section, only 128 images are used to calibrate a linear mapping of gray scale to phase shift to produce the LUT. This discrepancy is due to the fact that the most significant bit of the addressing scheme is actually a sign bit used to electrically balance the LC modulator to prevent ion migration and space charge build up at the electrodes. However, the nematic LC modulator is not sensitive to the polarity of the addressing field. Thus, the addressing values that range from 0 to 127 produce the same phase shift as the values 255 to 127, as shown in Figure 9. Therefore only 128 images that increase from gray values 0 to 127 are required in the calibration of the LUT for a device.

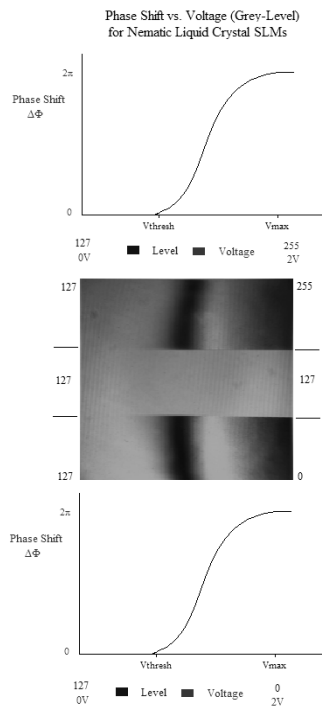


Figure 9 Example phase response of a phase SLM with respect to gray level

5. WAVEFRONT COMPENSATION APPLICATION AND TEST RESULTS

Using a fringe analysis program, the SLM is analyzed and a list of 20 Zernike polynomials is generated. The calibration software reads in that list of Zernike polynomials and generates a compensation image using equations that convert Zernike polynomials from polar coordinates to Cartesian coordinates. This image is superimposed with the desired phase image by adding the grayscale values of the two images pixel by pixel modulo 256. The resulting image is then processed through the LUT (look up table) that maps gray values 0 to 255 to a data set that results in a linear 0 to 2π phase shift. This image is then downloaded to the SLM. This process is outlined in the flow chart illustrated in Figure 10. The final result is an adaptive wavefront controller with only a quarter-wave ($\lambda/4$) of distortion and a linear phase response from 0 to 2π in the case of Device 1 (refer to Figure 1 and Figure 2).

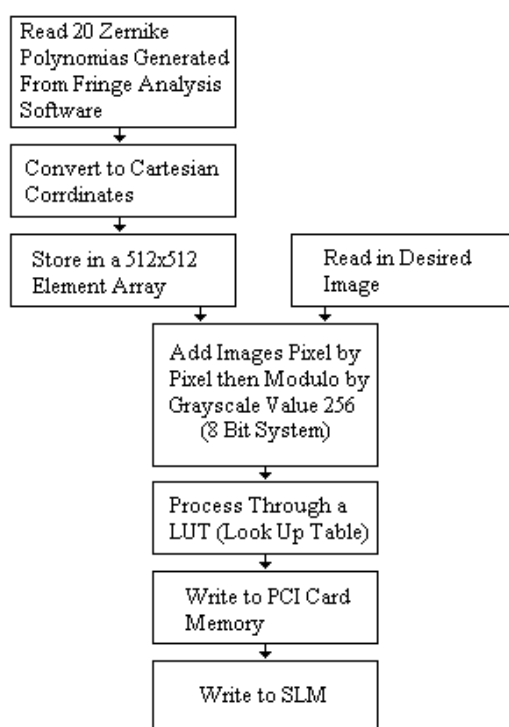


Figure 10 Wavefront distortion compensation Image Application Flow Chart

As an exercise in understanding the degree of compensation that can be achieved using the wavefront distortion compensation, a more severe example is looked at using Device 2 in Figure 11 and Figure 12. In this example, the wavefront distortion is approximately 2λ at 690nm before compensation Figure 11. The wavefront distortion after compensation is reduced to approximately $\lambda/2$ at 690nm which is demonstrated in Figure 12.

Device 2 before wavefront distortion compensation 2? (2 waves)

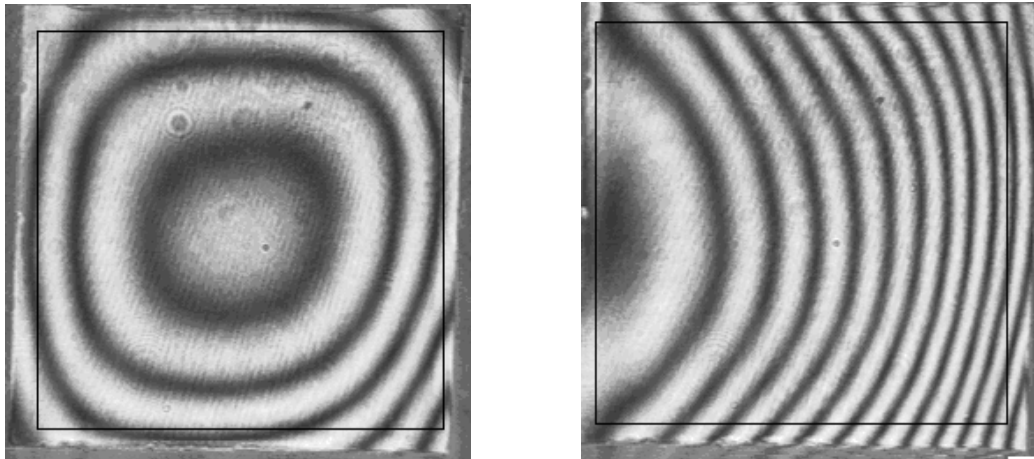


Figure 11 512 x 512 phase SLM, Device 2 before wavefront distortion compensation with no tilt (left) and x-tilt (right). The wavefront distortion of this device is approximately 2? (2 waves) at 690nm

Device 2 after wavefront distortion compensation ~.5? (half wave) over a circular aperture

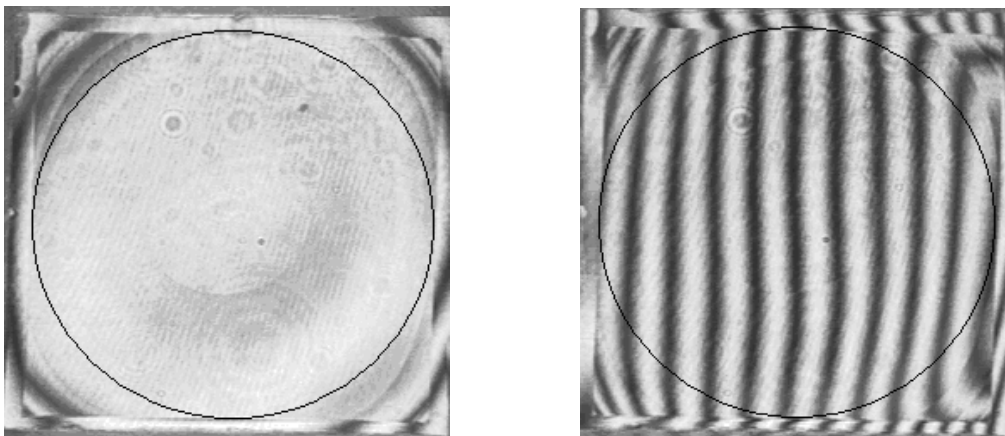


Figure 12 512 x 512 SLM, Device 2, after wavefront distortion compensation with no tilt (left) and x-tilt (right). The wavefront distortion of this device is approximately $\lambda/2$ (1/2 wave) analyzed over a circular aperture at 690nm

When comparing Device 1 to Device 2 it is clear that the wavefront distortion of Device 1 after compensation is less than that of Device 2. Not only does Device 1 have less wavefront distortion across the center of the device, but also it has significantly less distortion in the corner regions of the device. This is because Zernike polynomials define a wavefront over a circular aperture. The format of the SLMs is a two dimensional (2-D) square pixel array and because of this it would be ideal if Zernike polynomials defined a wavefront over a square aperture. Forcing a circular aperture to apply to a square aperture causes problems in the corners of the square. So, as the severity of the distortion of the device increases as it does in Device 2, it becomes increasingly difficult to accurately compensate in the corners of the device. This is clearly shown in Figure 12 where the corners of Device 2 have a distortion of approximately 2 waves. However, the wavefront distortion across the circular aperture in the center of Device 2 is approximately a half wave ($\lambda/2$). Although the wavefront distortion of Device 2 could not be compensated to the degree that Device 1 was, the wavefront

distortion of the device still saw a significant improvement - by a factor of four. Again this example is a useful illustration for examining how much distortion a device and system can have and still be compensated to some minimum threshold.

A quick test to verify a successful compensation and LUT calibration can be done by applying the compensation to an SLM and writing a phase pattern as shown in Figure 13, while using the calibrated LUT.

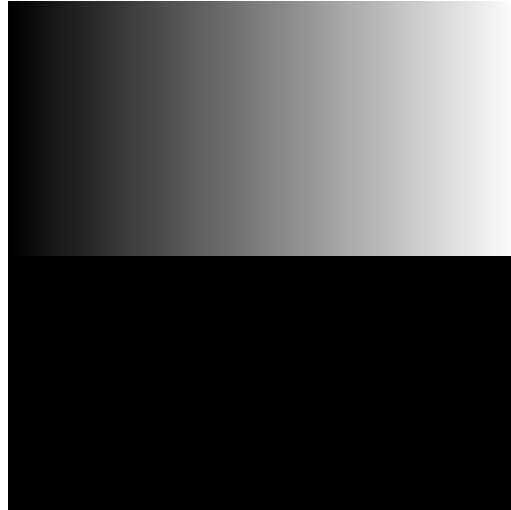


Figure 13 512 x 512 image with a gradient of gray values from 0 to 255 across the top half of the image and gray value 0 across the bottom half of the image.

When applying the compensation and the calibrated LUT, the wavefront distortion should decrease and the phase shift visible across the device in X should be linear and precisely 0 to 2π (refer to Figure 14).

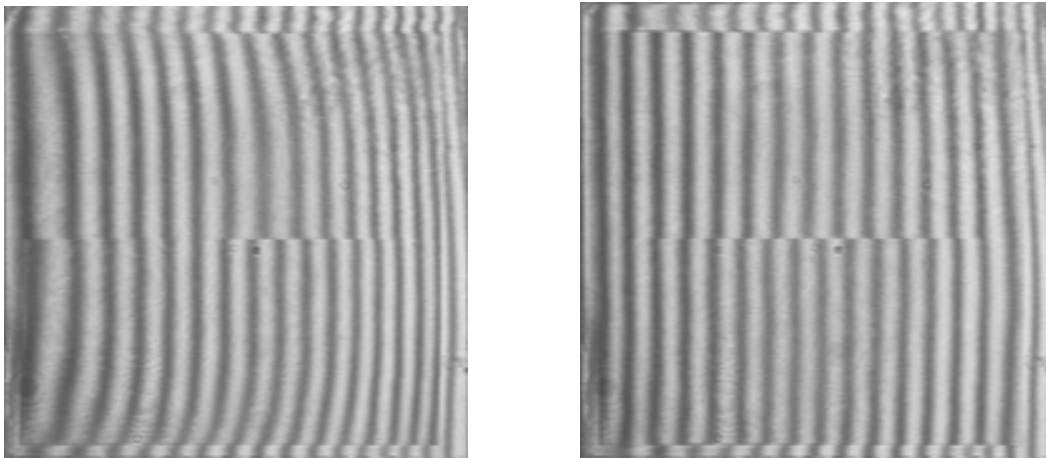


Figure 14 512 x 512 phase SLM, Device 1. The left image is an interferogram of device before compensation and before LUT calibration. The interferogram on the right is after compensation with the calibrated LUT.

The compensation image used to reduce the wavefront distortion reflected from the SLM can be applied to the SLM while also applying additional phase patterns to correct for other aberrations in a phase-only system. As shown in the flow chart of Figure 10, the compensation image is applied using modulo- 2π addition to any desired dynamic phase pattern and then written to the SLM by the control software. As represented by captured fringe patterns shown in

Figure 15, the compensation image and the dynamic phase patterns generated based on Zernike polynomial inputs accurately control the phase front producing clean representations of the desired wavefront.

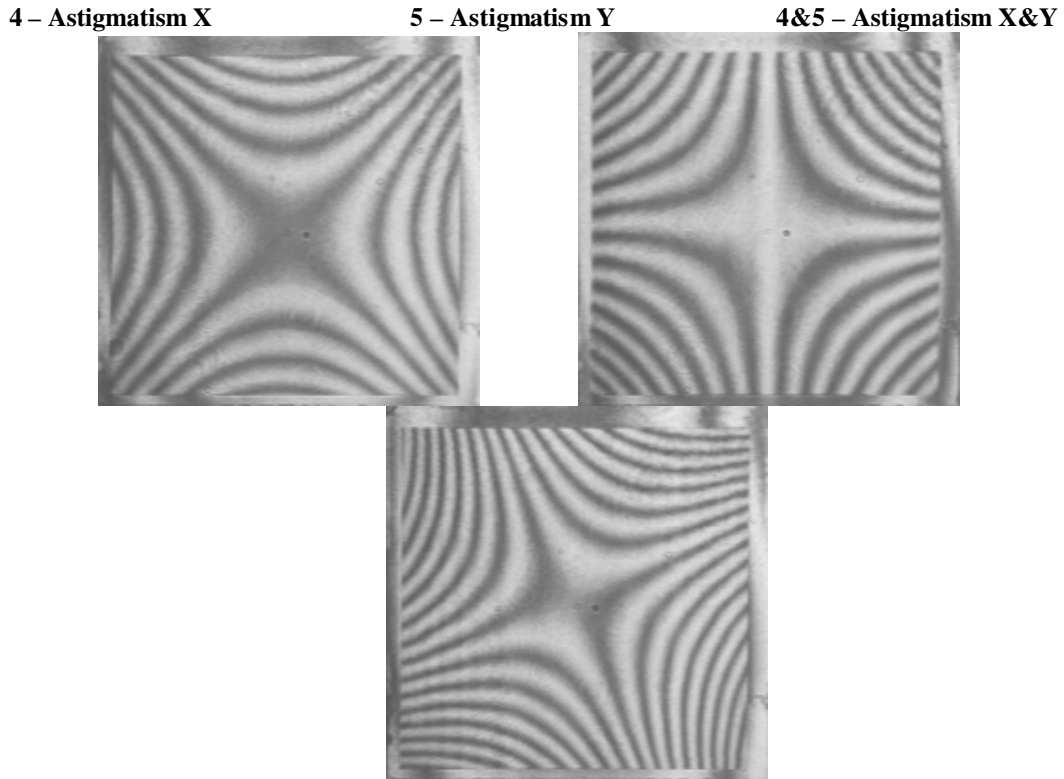


Figure 15 512 x 512 phase SLM, Device 1. After compensation and with Astigmatism X, Astigmatism Y, and Astigmatism X and Astigmatism Y, the fourth, fifth and fourth and fifth (combined) Zernike Polynomials, images loaded onto the SLM.

6. CONCLUSION

Techniques for analyzing and calibrating high-resolution liquid crystal phase SLMs have been discussed. These automated calibration techniques produce very good results when the phase SLM aberrations are not severe (less than a few waves). For severely distorted devices, the techniques can be less effective because there is greater zonal variation in the liquid crystal's phase response versus voltage. Fortunately, these techniques still offer a significant improvement in device performance as well as a more practical and user friendly technique of analyzing and calibrating phase LCoS SLMs.

ACKNOWLEDGEMENTS

This work was funded internally and through DARPA's Bio-Optic Synthetic Systems (BOSS) program.

REFERENCES

1. M. Giles, A. Seward, M.A. Vorontsov, J. Rha and R. Jimenez, "Setting up a liquid crystal phase screen to simulate atmospheric turbulence," *High-Resolution Wavefront Control: Methods, Devices, and Applications II, Proc. SPIE*, Vol. 4124 (2000)
2. G.D. Love, et al, "Emulating Multiconjugate Turbulence," *Beyond Conventional Adaptive Optics, Proc. ESO* (2001)

3. M. Gruneisen, et al, "Holographic correction in mid-IR using OA LC SLM elements," *High-Resolution Wavefront Control: Methods, Devices, and Applications II, Proc. SPIE*, **Vol. 4124** (2000)
4. T. Martinez, D.V. Wick, and S.R. Restaino, "Foveated, wide field-of-view imaging system using a liquid crystal spatial light modulator," *Opt. Express* **8**, 555-560 (2001),
5. D.J. Cho, S.T. Thurman, J.T. Donner and G.M. Morris, "Characterization of a 128x128 liquid-crystal spatial light modulator for wave-front generation," *OPTICS LETTERS*, **Vol. 23**, No. 12, 969-971 (1998).
6. X. Xun and R.W.Cohn, "Phase Calibration of spatially nonuniform spatial light modulators," *submitted for publication June, 2004*.